# Metal–Nitroxyl Interactions. 3.
# Spin-Labeled Copper Salicylaldimines

## D. L. DuBois,[1a] G. R. Eaton,*[1a] and S. S. Eaton[1b]

*Contribution from the Department of Chemistry, University of Denver, Denver, Colorado 80208, and the Department of Chemistry, University of Colorado at Denver, Denver, Colorado 80202. Received September 14, 1977*

**Abstract:** Resolved electron–electron coupling was observed in the room temperature solution EPR spectra of copper salicylaldimine complexes spin-labeled with 2,2,5,5-tetramethylpyrroline-1-oxyl. Values of the coupling constant vary with solvent ($CH_2Cl_2$, THF, 1:1 THF–$CH_2Cl_2$) and ring substituent (H, 5-*tert*-butyl) with values from 4.8 (0.000 46 cm$^{-1}$) to 11.8 G (0.0011 cm$^{-1}$) for the systems studied.

## Introduction

Application of the nitroxyl spin-label or spin probe techniques[2] to systems containing paramagnetic transition metal species requires analysis of the effect of the transition metal on the electron paramagnetic resonance (EPR) spectrum of the nitroxyl radical. It can be anticipated that both dipolar and exchange interactions between the paramagnetic transition metal and the nitroxyl radical could affect the EPR spectra. We are investigating a wide range of discrete transition metal complexes containing nitroxyl radicals to ascertain the relative contributions of dipolar and exchange interactions to the EPR spectra.[3-5] We have recently reported resolved spin–spin exchange interactions in a spin-labeled copper porphyrin[4] and in a complex of bis(hexafluoroacetylacetonato)copper(II) with nitroxyl-containing ligands which coordinate via a pyridine group.[5] In the present paper we report the preparation and EPR study of two new spin-labeled metal complexes (I and II),
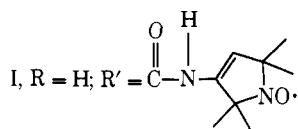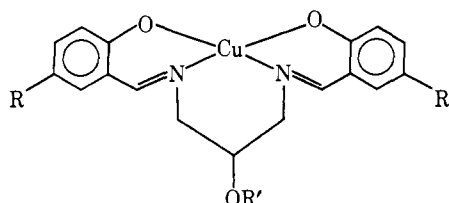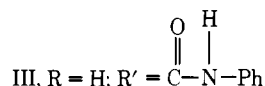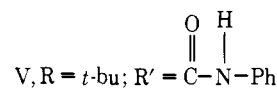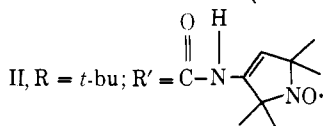


containing tetradentate salicylaldimine Schiff base type ligands.

## Experimental Section

**Physical Measurements.** All spectra were obtained in dry, purified solvents. Infrared spectra were recorded in Nujol mulls on a Perkin-Elmer 337 grating spectrometer. Visible spectra were obtained in dichloromethane, tetrahydrofuran, and pyridine solutions on a Beckman Acta V spectrometer. Solutions (1.0–3.0 × 10$^{-3}$ M) were used in 1-cm, 1-mm, and 0.1-mm path length cells providing data at constant concentration. Data are given below with wavelengths in nanometers and log ε in parentheses. Magnetic susceptibilities were measured on a Bruker Faraday balance with 1-μg sensitivity using

$HgCo(SCN)_4$[6] and [$Ni(en)_3$]$S_2O_3$[7] as calibrants. Values of $\mu_{eff}$ in Bohr magnetons are given below with the diamagnetic correction[8] ($X^{dia}$) used in the calculations given in parentheses. A temperature-independent paramagnetism (TIP) of 60 × 10$^{-6}$ was assumed for copper(II). This assumption is common, but in the few cases in which experimental estimates have been made, the TIP for copper(II) ranges from zero to 168 × 10$^{-6}$.[8] Thus the uncertainty in the correction may be about as large as the correction. Until temperature-dependent magnetic susceptibility data are available for these compounds the significance of the difference between the room temperature susceptibilities and the values expected for magnetically dilute systems cannot be assessed. EPR spectra were obtained on a Varian E-9 spectrometer using an E-231 cavity containing the quartz Dewar of the E-257 variable temperature accessory. The spectrometer is interfaced to a Varian 620/L-100 computer permitting data manipulation with the CLASS language.[9] Spectra were run on 5 × 10$^{-4}$ to 3 × 10$^{-3}$ M solutions at power levels below saturation and modulation amplitudes which did not cause line broadening. The g values were measured by means of the "marker" mode of the Varian E-272B field-frequency lock, which puts a mark on the spectrum at the zero-crossing point of the derivative spectrum of DPPH. The calibration of the field difference between DPPH in the cavity and the DPPH in the E-272B accessory was reproducible to within ±0.05 G on different days. All coupling constants are given in gauss (1 G = 0.1 mT).

**Preparation of Compounds. 3-Isocyanato-2,2,5,5-tetramethylpyrroline-1-oxyl (VII).** Pyridine (5 mL) was added to a slurry of 3-carboxy-2,2,5,5-tetramethylpyrroline-1-oxyl (4.36 g) in benzene (50 mL). The slurry was cooled in an ice bath and thionyl chloride (5 mL) was added dropwise. When the addition was complete, the reaction mixture was warmed to room temperature and stirred for 2 h. The reaction mixture was filtered, the residue was washed with benzene (10 mL), the filtrate and washings were combined, and the solvent was removed in vacuo from the combined solutions to yield an orange oil (which sometimes solidified). The product was dissolved in acetone (30 mL) and added dropwise to a cold (5–10 °C) aqueous solution of sodium azide (4.5 g/50 mL). The reaction mixture was stirred at 10–15 °C for 2 h and then extracted with four 50-mL portions of cold benzene. The extract was dried over 4 Å molecular sieves in a refrigerator overnight. The sieves were removed by filtration and the filtrate was refluxed for 24 h. The volume was reduced to ca. 10 mL by distillation at atmospheric pressure and the remaining benzene was removed in vacuo. The resultant yellow-orange oil solidified after cooling at 4 °C for 2 h. The product was purified by sublimation under vacuum using a hot water bath, yield 2.31 g (53%). Since the acid chloride intermediate and the product are moisture sensitive this preparation and all reactions utilizing the product were carried out under dry $N_2$ using Schlenk techniques: mp 44.0–44.5 °C, under $N_2$; IR $\nu_{N=C=O}$ 2270 cm$^{-1}$; EPR g = 2.0060, $\langle a \rangle_N$ = 14.2; $\mu_{eff}$ = 1.69 $\mu_B$ (measured at 27 °C, $X^{dia}$ = −96.1 × 10$^{-6}$). Anal. Calcd for $C_9H_{13}N_2O_2$: C, 59.65; H, 7.23; N, 15.46. Found: C, 59.74; H, 7.40; N, 15.70.

**(2-(N-(3-2,2,5,5-Tetramethylpyrroline-1-oxyl)carbamato)-N,N'-bis(salicylaldiminato)-1,3-diaminopropane)copper(II) (I).** VII (0.36 g, 2 mmol) was added to a slurry of 0.36 g (1 mmol) of IV[10] in 75 mL of THF. The reaction mixture was refluxed for 16 h, then cooled to room temperature. The green precipitate was filtered off, washed with two 5-mL portions of THF, and dried in vacuo for 12 h:

yield 0.37 g (68%); IR $\nu_{NH}$ 3170, $\nu_{C=O}$ 1735 cm$^{-1}$; $\mu_{eff}$ = 2.46 $\mu_B$ (measured at 27 °C, $X^{dia}$ = $-266.9 \times 10^{-6}$); visible spectrum (CH$_2$Cl$_2$ solution) 610 nm (2.41), 373 (4.09), 274 (4.45), 232 (4.76); (pyridine solution) 610 (2.29), 377 (4.06). Anal. Calcd for C$_{26}$H$_{29}$CuN$_4$O$_5$: C, 57.72; H, 5.40; N, 10.36. Found: C, 57.68; H, 5.32; N, 10.29.

**(2-(N-Methylcarbamato)-N,N'-bis(salicylaldiminato)-1,3-diaminopropane)copper(II) (III).** This complex was prepared in the same manner as I except that methyl isocyanate was used in place of VII: yield 41%; IR $\nu_{NH}$ 3240, $\nu_{C=O}$ 1715 cm$^{-1}$; $\mu_{eff}$ = 1.73 $\mu_B$ (measured at 27 °C, $X^{dia}$ = $-192.6 \times 10^{-6}$); visible spectrum (CH$_2$Cl$_2$ solution) 610 nm (2.46), 374 (4.07), 275 (4.45), 238 (4.67); (THF solution) 618 (2.44), 375 (3.96), 273 (4.33), 247 (4.54), 232 (4.63); (pyridine solution) 617 (2.32), 377 (4.15). Anal. Calcd for C$_{19}$H$_{19}$CuN$_3$O$_4$: C, 54.74; H, 4.59; N, 10.08. Found: C, 54.81; H, 4.69; N, 10.12.

**(2-Hydroxy-N,N'-bis(5-tert-butylsalicylaldiminato)-1,3-diaminopropanecopper(II) (VI).** This complex was prepared by the method reported for IV:[10] yield 90%; IR $\nu_{OH}$ 3200 cm$^{-1}$; $\mu_{eff}$ = 1.75 $\mu_B$ (measured at 28 °C, $X^{dia}$ = $-261.2 \times 10^{-6}$); visible spectrum (1:10 Me$_2$SO-CH$_2$Cl$_2$ solution) 610 nm (2.43), 380 (4.06); (1:10 Me$_2$SO-THF solution) 619 (2.49), 380 (4.09), 277 (4.45); (pyridine solution) 616 (2.42), 384 (4.06). Anal. Calcd for C$_{25}$H$_{32}$CuN$_2$O$_3$: C, 63.61; H, 6.83; N, 5.93. Found: C, 63.91; H, 7.08; N, 5.87.

**(2-(N-(3-2,2,5,5-Tetramethylpyrroline-1-oxyl)-carbamato)-N,N'-bis(5-tert-butylsalicylaldiminato)-1,3-diaminopropane)copper(II) (II).** VII (0.27 g, 1.5 mmol) was added to a slurry of 0.47 g (1.0 mmol) of VI in 70 mL of THF. The reaction mixture was refluxed for 16 h and the resultant green solution was filtered. The volume of the solution was reduced to ca. 10 mL on a rotary evaporator and 25 mL of diethyl ether was added. The green-brown microcrystalline product was collected on a frit and dried in vacuo: yield 0.52 g (80%); IR $\nu_{NH}$ 3155, $\nu_{CO}$ 1715 cm$^{-1}$; $\mu_{eff}$ = 2.43 $\mu_B$ (measured at 28 °C, $X^{dia}$ = $-313.3 \times 10^{-6}$); visible spectrum (CH$_2$Cl$_2$ solution) 608 nm (2.51), 384 (4.10), 279 (4.53), 250 (4.72), 229 (4.81); (THF solution) 618 (2.49), 384 (4.00), 275 (4.41), 250 (4.62), 233 (4.79); (pyridine solution) 610 (2.35), 386 (4.06). Anal. Calcd for C$_{34}$H$_{45}$CuN$_4$O$_5$: C, 62.51; H, 6.94; N, 8.58. Found: C, 62.67; H, 7.09; N, 8.42.

**(2-(N-Phenylcarbamato)-N,N'-bis(5-tert-butylsalicylaldiminato)-1,3-diaminopropane)copper(II) (V).** This compound was prepared analogously to II except that phenyl isocyanate was used in place of VII: yield 44%; IR $\nu_{NH}$ 3245, $\nu_{CO}$ 1710 cm$^{-1}$; $\mu_{eff}$ = 1.74 $\mu_B$ (measured at 28 °C, $X^{dia}$ = $-319.1 \times 10^{-6}$); visible spectrum (CH$_2$Cl$_2$ solution) 609 nm (2.50), 384 (4.06), 279 (4.50), 234 (4.81); (THF solution) 618 (2.48), 385 (3.98), 275 (4.40), 235 (4.79); (pyridine solution) 611 (2.35), 385 (4.05). Anal. Calcd for C$_{32}$H$_{37}$CuN$_3$O$_4$: C, 65.01; H, 6.31; N, 7.11. Found: C, 64.79; H, 6.52; N, 6.92.

**Computer Simulations.** The EPR spectra of the copper complexes with diamagnetic ligands (III, V, VI) were simulated using a computer program which included first-order nitrogen hyperfine coupling, first-order Breit-Rabi corrections,[11] dependence of intensity on $g$ value,[12] and line widths that varied with the copper nuclear spin as $A + Bm_1 + Cm_1^2$.[13] The principal features of the program used to simulate the EPR spectra of the spin-labeled copper complexes are outlined below, with details provided elsewhere.[14] The electron-electron coupling is analogous to the AB pattern commonly found in high-resolution NMR.[15] Since the copper nuclear spin and nitroxyl nitrogen spin must also be included in the spin system it is an ABMX-type system.[15] The effect of coupling to the copper nucleus, the two nitrogens in the copper coordination sphere, and the nitroxyl nitrogen were included using the "X approximation".[15] Corrections were made for the dependence of intensity on $g$ value[12] and for the field dependence of the energy separation between copper and nitroxyl energy levels. Breit-Rabi corrections[11] were included for the copper nucleus coupling. In the following discussions transitions are labeled as "copper" or "nitroxyl" according to the nature of the transition as $J \rightarrow 0$. The line widths of the "copper lines" were assumed to vary as $A + Bm_1 + Cm_1^2$ where $m_1$ is the copper nuclear spin. Line widths of the "nitroxyl lines" were assumed to vary as $A + Bm_1 + Cm_1^2$ where $m_1$ is the nitroxyl nitrogen nuclear spin. Different line width parameters can be input for the "inner" and "outer" lines of the AB quartets. Both $^{63}$Cu and $^{65}$Cu were included in all calculations.

**Results and Discussion**

The copper complexes I–III and V were prepared by the reaction of isocyanates with the alcohol group in IV and VI

yielding substituted carbamates. The IR of the products lacks the OH stretch characteristic of IV and VI and includes instead the NH and CO stretches characteristic of substituted carbamates. The products are stable in the solid phase when stored in a desiccator. Slow decomposition occurs in solution.

**Magnetic Susceptibility.** The solid state magnetic moments of the copper complexes with diamagnetic ligands, III and V, are 1.73 and 1.74 $\mu_B$, respectively, which is reasonable for Cu(II) with a small orbital contribution.[8] The solid state magnetic moments for the spin-labeled copper complexes I and II are 2.46 and 2.43 $\mu_B$, respectively. Since a spin-only value of $\sqrt{2} \times 1.73$ or 2.44 $\mu_B$ would be expected for two independent electrons, assuming no orbital contribution, the susceptibility data for the spin-labeled copper complexes are consistent with very small ($\ll kT$) interaction between the copper and nitroxyl electrons in the solid phase. Further interpretation of the solid state magnetic susceptibility data must await variable temperature data.

**Electronic Spectra.** The visible and ultraviolet spectra of I–III, V, and VI are given in the Experimental Section. Since the EPR spectra (see below) indicated greater decomposition in more dilute solutions, all UV–vis spectra were run at ca. 10$^{-3}$ M concentrations using cells with 0.1-mm to 1.0-cm path lengths. In CH$_2$Cl$_2$ solution all the complexes have a d–d transition at 608–610 nm as has been previously observed for IV[10] and VIII.[16] The higher intensity bands in the electronic spectra which occur between 220 and 400 nm are very similar for the spin-labeled copper complex I and the closely related III. Likewise, except for the contribution of the phenyl ring in V, the spectra of II and V between 220 and 400 nm are very similar. The close similarities between the electronic spectra of the spin-labeled copper complexes and the unlabeled analogues suggest that the structure of the copper complexes is not strongly perturbed by the spin labeling.

The effect of solvent on the d–d band was examined for CH$_2$Cl$_2$, THF, and pyridine solutions of II, III, V, and VI, and in CH$_2$Cl$_2$ and pyridine for I. (I is only sparingly soluble in THF.) In each case the d–d band occurs at lower energy in THF solution than in CH$_2$Cl$_2$. In pyridine the energy of the transition is intermediate between the values in CH$_2$Cl$_2$ and THF solutions. Shifts in the band to lower energy may be due to weak coordination of a fifth ligand and/or slightly greater distortion away from planarity at the copper.[17]

**EPR Spectra.** The EPR spectra of the copper complexes with diamagnetic ligands show the familiar four-line pattern due to coupling to the copper nucleus ($I = \frac{3}{2}$), with line widths decreasing to high field. Poorly resolved superhyperfine coupling to the two nitrogens in the copper coordination sphere is observed for the highest field line. The spectrum of III in CH$_2$Cl$_2$ is given in Figure 1A. Line width and coupling parameters obtained by computer simulation of the spectra are given in Table I. Coupling to other nuclei in the molecule may be present, but is not resolved in the spectra, so it is treated in the simulations only as line broadening.

The EPR spectrum of the spin-labeled copper complex, I, in CH$_2$Cl$_2$ solution is shown in Figure 1B. An expanded presentation of the "nitroxyl" portion of the spectrum is given in Figure 2A. If there were no interaction between the copper and nitroxyl electrons, a superposition of the four-line copper spectrum and a three-line nitroxyl spectrum (coupling to 1 N, $I = 1$) would be expected. However, the "nitroxyl" region is clearly not a usual three-line pattern. As seen by the similarity between the observed and calculated spectra in Figures 1 and 2A the changes in the "copper" and "nitroxyl" spectra are consistent with an electron-electron coupling constant, $J$, of 7.5 G (0.000 72 cm$^{-1}$). Since $J$ is smaller than the nitrogen hyperfine coupling (14.5 G, 0.0013 cm$^{-1}$) the two nitroxyl triplets are largely superimposed. A small amount of free nitroxyl due to decomposition can also be seen in the spectrum.

**Table I.** EPR Spectra of Copper Complexes with Diamagnetic Ligands

| Complex | Solvent | Concn | $g^a$ | $\langle a \rangle_{Cu}$,[b] G | $\langle a \rangle_{N}$,[c] G | $A^d$ | $B^d$ | $C^d$ |
|---------|---------|-------|-------|-----------------|-----------------|-------|-------|-------|
| III | $CH_2Cl_2$ | $1.0 \times 10^{-3}$ | 2.1059 | 77.2 | 13.2 | 23.1 | 7.5 | 1.6 |
| III | 1:1 THF–$CH_2Cl_2$ | $1.7 \times 10^{-3}$ | 2.1068 | 75.9 | 13.4 | 23.6 | 8.7 | 1.8 |
| V | 1:1 THF–$CH_2Cl_2$ | $1.9 \times 10^{-3}$ | 2.1051 | 74.9 | 13.6 | 26.1 | 14.3 | 3.3 |
| V | THF | $1.1 \times 10^{-3}$ | 2.1087 | 74.3 | 13.2 | 25.7 | 13.6 | 2.9 |
| VI | 1:1 THF–$CH_2Cl_2$ | $1.9 \times 10^{-3}$ | 2.1069 | 74.9 | 13.4 | 22.6 | 10.2 | 2.3 |

[a] Uncertainty ±0.0007. [b] Uncertainty ±0.2. The value given is for $^{63}Cu$. The value for $^{65}Cu$ is 1.07 × the value given. [c] Uncertainty ±0.2. [d] $A$, $B$, and $C$ are the line width parameters; see text. Values given are for 100% Lorentzian lines.
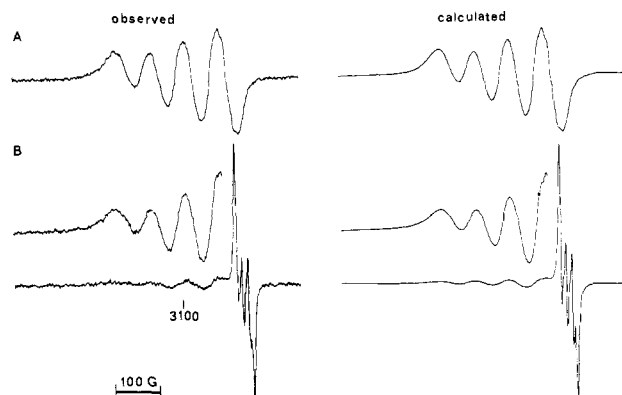


**Figure 1.** X-band (~9.11 GHz) EPR spectra in $CH_2Cl_2$ solution and computer simulations: (A) copper complex, III, 650 G scan, 125 G/min scan rate, 40 mW, 1.25 G modulation amplitude; (B) spin-labeled copper complex, I, full spectrum 650 G scan, 125 G/min scan rate, 10 mW, 0.20 G modulation amplitude; expanded "copper" region, 500 G scan, 125 G/min scan rate, 40 mW, 1.0 G modulation amplitude. Additional parameters are given in Tables I and II.
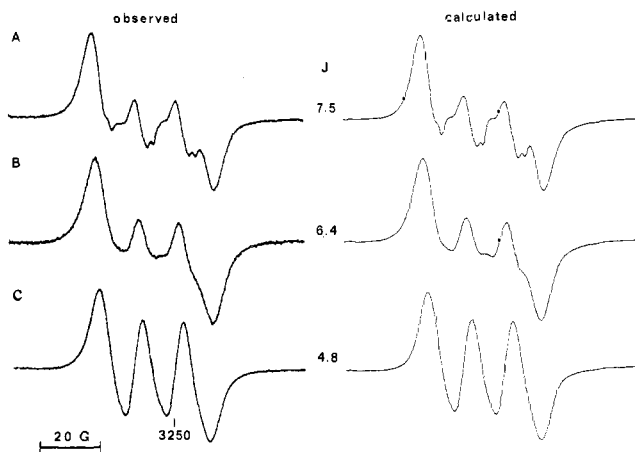


**Figure 2.** "Nitroxyl" region of the X-band (~9.11 GHz) EPR spectra of I as a function of solvent, and computer simulations: (A) $CH_2Cl_2$ solution, 100 G scan, 12.5 G/min scan rate, 10 mW, 0.20 G modulation amplitude; (B) THF solution, 100 G scan, 12.5 G/min scan rate, 10 mW, 0.63 G modulation amplitude; (C) 1:1 THF–$CH_2Cl_2$ solution, 100 G, 12.5 G/min scan rate, 20 mW, 0.20 G modulation amplitude. Values of the electron–electron coupling constant, $J$, are given in gauss. Additional parameters are given in Tables I and II.

The $g$ values for the metal and nitroxyl electrons in the spin-labeled copper complex appear to be unchanged from the values in the copper complex, III and the nitroxyl, VII, re-
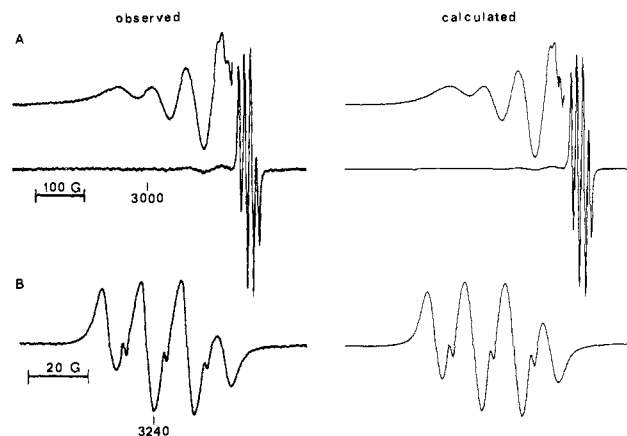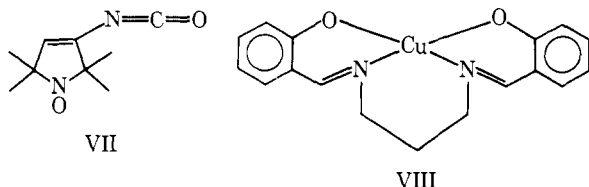


**Figure 3.** X-band (~9.11 GHz) EPR spectra of the spin-labeled copper complex, II, in THF solution, and computer simulation: (A) full spectrum, 650 G scan, 125 G/min scan rate, 10 mW, 0.16 G modulation amplitude; expanded "copper" region, 500 G scan, 125 G/min scan rate, 40 mW, 2.0 G modulation amplitude; (B) "nitroxyl" region, 100 G scan, 25 G/min scan rate, 10 mW, 0.16 G modulation amplitude. Additional parameters are given in Tables I and II.

spectively. The line widths for both the "copper" and "nitroxyl" transitions in I are slightly broader than in III and VII, respectively. Further, the "outer nitroxyl" lines are slightly broader than the "inner nitroxyl" lines of the AB pattern. The "copper" lines are too broad to tell if there are line width differences between the "inner" and "outer" lines. Values for the line width and coupling parameters are given in Table II.

The value of $J$ is solvent dependent as shown by the spectra in Figure 2, varying from 4.8 G (0.000 46 cm$^{-1}$) in 1:1 THF–$CH_2Cl_2$ to 7.5 G (0.000 72 cm$^{-1}$) in $CH_2Cl_2$. It is not obvious why the electron–electron coupling is smaller in 1:1 THF–$CH_2Cl_2$ than in either THF or $CH_2Cl_2$ alone.

The EPR spectra of II (Figure 3) indicate that substituents on the salicylaldimine ring can influence the magnitude of $J$. In II the electron–electron coupling is substantially larger, 11.8 G (0.0013 cm$^{-1}$) in THF, than it is in I. In this case $J$ is almost as large as $\langle a \rangle_N$ so the nitroxyl region looks approximately like a four-line pattern. Further studies are in progress to elucidate the effects of other solvents and substituents on the electron–electron coupling in these systems.

EPR microwave power saturation studies also dramatically demonstrate metal–nitroxyl interactions. In the absence of saturation effects a plot of signal amplitude vs. the square root of the microwave power, $P^{1/2}$, is linear. Linear amplitude vs. $P^{1/2}$ plots were obtained for the copper EPR lines for all of the complexes studied. The amplitude vs. $P^{1/2}$ plot for the isocyanate nitroxyl VII deviated from linearity above ca. 1 mW for a $6.7 \times 10^{-5}$ M solution and above ca. 2 mW for a $1.7 \times 10^{-3}$ M solution, the difference presumably being due to collision-induced relaxation. The data yield $P_{1/2}$ = 30 and 58 mW, respectively. $P_{1/2}$ is the power at which the EPR signal amplitude is half as great as it would be had no saturation occurred. The

VII

VIII

**Table II**

| Complex | Solvent | Concn | $J$ $(G)$, cm$^{-1}$ | $\langle a \rangle_{Cu}$,[a] G | $\langle a \rangle_N$,[b] G | $\langle a \rangle_N$,[c] G | Line width parameters[d] | | |
|---|---|---|---|---|---|---|---|---|---|
| | | | | | | | A | B | C |
| I | CH$_2$Cl$_2$ | $1.1 \times 10^{-3}$ | 7.5 (0.000 72) | 76.9 | 13.2 | 14.5 | Cu 24.6<br>NO(i) 6.7<br>NO(o) 7.25 | 10.2<br>0.05<br>0.05 | 1.6<br>−0.05<br>0.0 |
| I | THF | $5.0 \times 10^{-4}$ | 6.4 (0.000 61) | 74.0 | 13.4 | 14.3 | Cu 24.6<br>NO(i) 7.45<br>NO(o) 7.7 | 10.2<br>0.13<br>0.1 | 1.6<br>−0.08<br>0.0 |
| I | 1:1 THF-CH$_2$Cl$_2$ | $1.5 \times 10^{-3}$ | 4.8 (0.000 46) | 75.0 | 13.4 | 14.5 | Cu 25.8<br>NO(i) 6.8<br>NO(o) 7.3 | 11.6<br>0.1<br>0.1 | 2.1<br>0.0<br>0.0 |
| II | THF | $9.5 \times 10^{-4}$ | 11.8 (0.001 1) | 72.7 | 13.2 | 14.4 | Cu 30.1<br>NO(i) 5.2<br>NO(o) 5.7 | 16.3<br>0.0<br>0.0 | 3.6<br>0.0<br>0.0 |
| II | 1:1 THF-CH$_2$Cl$_2$ | $1.8 \times 10^{-3}$ | 11.1 (0.001 0) | 73.4 | 13.4 | 14.5 | Cu 30.4<br>NO(i) 5.2<br>NO(o) 5.7 | 16.5<br>0.0<br>0.0 | 3.5<br>0.0<br>0.0 |

[a] Value given is for $^{63}$Cu. [b] Coupling of copper electron to two nitrogens in copper coordination sphere. [c] Coupling of nitroxyl electron to nitroxyl nitrogen. [d] Values given for "copper" and "nitroxyl" lines are $A$, $B$, and $C$ in formula $A + Bm_1 + Cm_1^2$. (i) and (o) denote "inner" and "outer" nitroxyl lines. "Copper" line shapes are 100% Lorentzian and "nitroxyl" line shapes are 50% Lorentzian and 50% Gaussian.

$P_{1/2}$ values are not corrected for the modulation and power nonuniformities discussed by Hyde and co-workers.[18] In the *t*-Bu-substituted copper–nitroxyl complex, II, no indication of saturation of the "nitroxyl" lines was observed at power levels up to 200 mW (the highest power attainable on the E-9 spectrometer). The "nitroxyl" lines of complex I exhibited some saturation above ca. 20–40 mW, though not enough to estimate $P_{1/2}$ (the deviation was ~13% at 200 mW). Clearly the copper–nitroxyl interaction has a major impact on the relaxation of the "nitroxyl" electron.

The values of the parameters in Table II were obtained by visual comparison of calculated and observed spectra. The "copper" lines are so broad that the simulated spectra of these lines are rather insensitive to $\langle a \rangle_N$ and $J$. Thus the value of $\langle a \rangle_N$ observed for the related complexes with diamagnetic ligands was used in the simulations. The copper hyperfine coupling is clearly resolved and was adjusted to fit the observed spectra. The values of $\langle a \rangle_{Cu}$ obtained were similar to those observed for the related complexes with diamagnetic ligands. The value of $J$ was obtained from the "nitroxyl" lines. When the value of $J$ is about half the value of the nitroxyl $\langle a \rangle_N$ as in I, there is extensive overlap of lines, but different features of the spectra are controlled by $\langle a \rangle_N$ and $J$ so that accurate values of $\langle a \rangle_N$ ($\pm 0.1$ G) and $J$ ($\pm 0.2$ G) can be obtained. However, as $J$ approaches $\langle a \rangle_N$, as in II, the relative effects of $\langle a \rangle_N$ and $J$ on the simulated spectra are less distinctive and there is more uncertainty ($\langle a \rangle_N$, $\pm 0.2$ G; $J$, $\pm 0.4$ G) although the sum $J + 2\langle a \rangle_N$ is determined by the positions of the outside lines.

**Comparison with Prior Results.** The values of $J$ observed in these systems are substantially smaller than those observed for a spin-labeled copper porphyrin (0.0072 cm$^{-1}$)[4] and in a spin-labeled adduct of copper bis(hexafluoroacetylacetonate) (0.0042 cm$^{-1}$).[5]

**References and Notes**

(1) (a) University of Denver; (b) University of Colorado at Denver.
(2) (a) G. I. Likhtenshtein, "Spin Labeling Methods in Molecular Biology", Wiley, New York, N.Y., 1976; (b) L. J. Berliner, Ed., "Spin Labeling", Academic Press, New York, N.Y., 1976.
(3) G. R. Eaton, *Inorg. Nucl. Chem. Lett.*, **8**, 647 (1972).
(4) G. A. Braden, K. T. Trevor, J. M. Neri, D. J. Greenslade, G. R. Eaton, and S. S. Eaton, *J. Am. Chem. Soc.*, **99**, 4854 (1977).
(5) P. M. Boymel, J. R. Chang, D. L. DuBois, D. J. Greenslade, G. R. Eaton, and S. S. Eaton, *J. Am. Chem. Soc.*, **99**, 5500 (1977).
(6) B. N. Figgis and R. S. Nyholm, *J. Chem. Soc.*, 4190 (1958); H. St. Rade, *J. Phys. Chem.*, **77**, 424 (1973).
(7) N. F. Curtis, *J. Chem. Soc.*, 3147 (1961).
(8) (a) A. Earnshaw, "Introduction to Magnetochemistry", Academic Press, New York, N.Y., 1968, pp 5–7; (b) E. A. Boudreaux and L. N. Mulay, Ed., "Theory and Applications of Molecular Paramagnetism", Wiley, New York, N.Y., 1976; (c) B. N. Figgis and C. M. Harris, *J. Chem. Soc.*, 855 (1959); (d) R. L. Martin and H. Waterman, *ibid.*, 2960 (1959).
(9) C. H. Klopfenstein, P. Jost, and O. H. Griffith, *Comput. Chem. Biochem. Res.*, 1, 176 (1972).
(10) K. Dey, *Indian J. Chem.*, **9**, 887 (1971).
(11) B. A. Goodman and J. B. Raynor, *Adv. Inorg. Chem. Radiochem.*, **13**, 224 (1970).
(12) R. Aasa and T. Vänngård, *J. Magn. Reson.*, **19**, 308 (1975).
(13) H. McConnell, *J. Chem. Phys.*, **25**, 709 (1956); D. Kivelson, *ibid.*, **33**, 1094 (1960).
(14) S. S. Eaton, D. L. DuBois, and G. R. Eaton, to be published.
(15) R. J. Abraham, "The Analysis of High Resolution NMR Spectra", American Elsevier, New York, N.Y., 1971, Chapters 3 and 6.
(16) R. H. Holm, *J. Am. Chem. Soc.*, **82**, 5632 (1960).
(17) H. Yokoi, *Bull. Chem. Soc. Jpn.*, **47**, 3037 (1974); H. Yokoi and A. W. Addison, *Inorg. Chem.*, **16**, 1341 (1977).
(18) C. Mailer, T. Sarna, H. M. Swartz, and J. S. Hyde, *J. Magn. Reson.*, **25**, 205 (1977).